

Silencing of TMED5 inhibits proliferation, migration and invasion, and enhances apoptosis of hepatocellular carcinoma cells

Xianyi Cheng^{A–F}, Xiulan Deng^{B,E,F}, Huiping Zeng^{C,D,F}, Tao Zhou^{C,E,F}, Dezhi Li^{A,D,F}, Wei V. Zheng^{A,D–F}

Intervention and Cell Therapy Center, Peking University Shenzhen Hospital, China

A – research concept and design; B – collection and/or assembly of data; C – data analysis and interpretation;

D – writing the article; E – critical revision of the article; F – final approval of the article

Advances in Clinical and Experimental Medicine, ISSN 1899–5276 (print), ISSN 2451–2680 (online)

Adv Clin Exp Med. 2023;32(6):677–688

Address for correspondence

Wei V. Zheng

E-mail: zhengw2013@yeah.net

Funding sources

This work was supported by the Sanming Project of Medicine in Shenzhen (grant No. SZSM201612071), the Cell Technology Center and Transformation Base, Innovation Center of Guangdong-Hong Kong-Macao Greater Bay Area, Ministry of Science and Technology of China (grant No. YCZYPT[2018]03-1), Shenzhen Key Discipline of Stem Cell Clinical Research (grant No. SZXK078), and the Scientific Research Foundation of Peking University Shenzhen Hospital (grant No. KYQD202100X).

Conflict of interest

None declared

Received on January 4, 2021

Reviewed on September 20, 2022

Accepted on November 17, 2022

Published online on December 19, 2022

Abstract

Background. Transmembrane P24 trafficking protein 5 (TMED5) is highly expressed in cervical and bladder cancer cell lines. Moreover, TMED5 promotes nuclear autophagy and the malignant behavior of cervical cancer cells. However, the role of TMED5 in hepatocellular carcinoma (HCC) has not been extensively reported.

Objectives. To investigate the role of TMED5 in HCC cells.

Materials and methods. Bioinformatics was used to analyze the messenger-ribonucleic acid (mRNA) expression of TMED5 in HCC and its relationship with overall survival and disease-free interval of HCC patients. After TMED5 was decreased in SMMC-7721 and Hep3B cells, they were assayed for proliferation, cell cycle, apoptosis, migration, and invasion.

Results. The expression of TMED5 mRNA in HCC tissues was higher than in adjacent normal tissues, and the overall survival of HCC patients with high TMED5 transcription levels was worse. Moreover, the overexpression of TMED5 was associated with HCC progression. The downregulation of TMED5 suppressed cell proliferation, migration and invasion, and enhanced apoptosis. Therefore, TMED5 may be involved in the regulation of the cell cycle, the mammalian target of rapamycin signaling pathway, and the transforming growth factor beta (TGF- β) signaling pathway.

Conclusions. The TMED5 has the potential to promote HCC progression. Therefore, lowering TMED5 levels could represent a potential strategy for the treatment of HCC.

Key words: proliferation, hepatocellular carcinoma, bioinformatic analysis, TMED5

Cite as

Cheng X, Deng X, Zeng H, Zhou T, Li D, Zheng WV. Silencing of TMED5 inhibits proliferation, migration and invasion, and enhances apoptosis of hepatocellular carcinoma cells. *Adv Clin Exp Med.* 2023;32(6):677–688. doi:10.17219/acem/156673

DOI

10.17219/acem/156673

Copyright

Copyright by Author(s)

This is an article distributed under the terms of the Creative Commons Attribution 3.0 Unported (CC BY 3.0) (<https://creativecommons.org/licenses/by/3.0/>)

Background

Hepatocellular carcinoma (HCC) is the most common form of liver cancer.¹ There are more than 700,000 new cases of HCC reported annually worldwide, which accounts for 9.2% of all new cancer cases, and more than 600,000 HCC patients die globally each year.¹ However, the early symptoms of HCC are not obvious.^{2,3} In this regard, the development of biomarkers that can be used for the early diagnosis of HCC is essential to improve the survival rate of HCC patients. Although biomarkers, such as alpha-fetoprotein (AFP), have been identified and used for clinical diagnosis, there is still a need to improve their specificity and sensitivity.⁴ Despite efforts to understand the molecular mechanisms that regulate the occurrence and development of HCC in recent decades,⁵ these mechanisms remain unclear.

Transmembrane P24 trafficking protein 5 (TMED5), also known as p28, is a newly discovered member of the γ sub-family of p24 membrane proteins.⁶ It is located in the endoplasmic reticulum, Golgi intermediate compartment and the cis-Golgi apparatus, and is involved in vesicle-mediated protein transport.⁶ It has been shown that the upregulation of TMED5 promotes nuclear autophagy and the malignant behavior of cervical cancer cells.⁷ In addition, TMED5 was found to be significantly overexpressed in the SCaBER cell line.⁸ These findings suggest that TMED5 is a potential target for certain types of cancer. However, little is known about the role of TMED5 in HCC.

Objectives

In this study, preliminary investigations into the role of TMED5 in HCC were conducted using bioinformatics analysis. The role of TMED5 in the proliferation, apoptosis, migration, and invasion of HCC cells was then explored using in vitro experiments.

Materials and methods

Bioinformatic analysis

Genes that are differentially expressed between HCC tissues and adjacent normal tissues from The Cancer Genome Atlas (TCGA; <https://portal.gdc.cancer.gov/>) were identified using the R package edgeR v. 3.30.3 (R Foundation for Statistical Computing, Vienna, Austria). A volcano map was then drawn with $p < 0.05$ and $|\log_2(\text{fold change})| > 1$ set as the threshold. The TMED5 messenger ribonucleic acid (mRNA) levels in paired and unpaired HCC tissues, and adjacent normal tissues, were retrieved from TCGA or Gene Expression Omnibus (<https://www.ncbi.nlm.nih.gov/geo/>) (GSE84005) and analyzed using the R package edgeR. The distinct expression of TMED5 was analyzed in 33 types of cancer retrieved from TCGA.

Hepatocellular carcinoma patients were divided into high- and low-expression groups based on the median value of their TMED5 levels. The overall survival (OS) and disease-free interval (DFI) were then calculated using the R package survminer v. 0.4.8 (R Foundation for Statistical Computing, Vienna, Austria), and the Kaplan–Meier survival curve was drawn. The TMED5 was combined with the tumor-node-metastasis (TNM) stage to construct a nomogram model, and a calibration curve was drawn to assess the accuracy of the model.

The clinical data of HCC patients extracted from TCGA were used for univariate and multivariate Cox proportional hazard regression.⁹ Cancer-related pathways associated with TMED5 levels in HCC were then used for gene set enrichment analysis (GSEA) using GSEA v. 4.0.0 software (Broad Institute and University of California San Diego, USA).

Cell culture and transfection

The L-02, Hep3B, HepG2, SMMC-7721, and Huh7 cells (catalog No. IM-H289, IM-H367, IM-H038, IM-H047, and IM-H040, respectively; IMMOCELL, Xiamen, China) were cultured in Dulbecco's modified Eagle's medium (catalog No. D0819; Sigma-Aldrich, St. Louis, USA), supplemented with 10% fetal bovine serum (FBS), 100 U/mL penicillin and 100 U/mL streptomycin (Gibco, Detroit, USA) at 37°C.

Three small interfering RNAs (siRNAs) targeting TMED5 were designed (Table 1) and obtained from Huzhou Hippo Biotechnology Co., LTD (HIPPOBIO; Huzhou, China). In total, 1×10^6 cells/well were seeded into 6-well plates. Then, siRNAs were transfected into cells using Lipofectamine 2000 (catalog No. 11668027; Invitrogen, Carlsbad, USA) at 100 pmol per well. Cells were collected for cell proliferation, apoptosis, migration, and invasion assays, as well as for western blotting analysis and quantitative polymerase chain reaction (qPCR) 48 h after transfection.

Table 1. The sequence of small interfering RNAs (siRNAs) of transmembrane P24 trafficking protein (TMED5)

Name	Sequence 5'-3'
siTMED5-1	AGAUGGAGUUCACACUGUAGATT
siTMED5-2	GAAGAUUGGAAGAAUAUUAUUTT
siTMED5-3	GAAACAUACAAGAAAGCAACUTT

Cell proliferation assays

To detect the effects of *TMED5* knockdown on cell proliferation, 3-(4,5-dimethylthiazol-2-yl)-2,5-diphenyltetrazolium bromide (MTT), cell cycle and colony formation assays were used. After treatment with siRNAs, SMMC-7721 and Hep3B cells were inoculated into a 96-well plate and incubated for 24 h, 48 h or 72 h. At each time point, 20 μ L of 5 mg/mL MTT reagent (catalog No. 40201ES72; Yeasen Biotechnology Co. Ltd., Shanghai, China) was added to each well of the plate according to the manufacturer's

instructions to test cell survival. Then, the absorbance was measured at 490 nm using a SpectraMax® Absorbance Reader (Molecular Devices, San Francisco, USA). The data are presented as the mean \pm standard deviation (M \pm SD) of sextuple wells.

After treatment with siRNAs, SMMC-7721 and Hep3B cells were seeded into 6-well plates at a density of 5×10^2 cells per well to perform the colony formation assay. When the colonies were visible to the naked eye, they were fixed with methanol for 15 min and stained with 0.5% crystal violet (catalog No. 60505ES25; Yeasen Biotechnology Co. Ltd.) in phosphate-buffered saline (PBS) for 15 min. Finally, the colonies were imaged and the numbers of colonies were counted using ImageJ 1.52v (National Institutes of Health, Bethesda, USA).

To examine the cell cycle, 1×10^6 siRNA-treated SMMC-7721 and Hep3B cells were fixed with pre-cooled 75% ethanol at 4°C for 4 h and then incubated with 0.2% Triton X-100 (catalog No. ST797; Beyotime Biotechnology, Shanghai, China) and 10 μ g/mL RNase A (catalog No. ST577; Beyotime Biotechnology) in PBS at 37°C for 30 min. Next, the cells were stained with 20 μ g/mL propidium iodide (PI) (catalog No. A211-01; Vazyme, Nanjing, China) and kept in the dark at 28°C for 30 min. The stained cells were then analyzed using a NovoCyte 1300 flow cytometer (ACEA Biosciences, San Diego, USA).

Apoptosis assay

After siRNA treatment, SMMC-7721 and Hep3B cells were harvested for apoptosis detection, which was performed using an Annexin V-fluorescein isothiocyanate (FITC)/7-amino-actinomycin D (7-AAD) Apoptosis Detection Kit (catalog No. A211-01; Vazyme), according to the manufacturer's instructions. Flow cytometry detection was then carried out on the cells (NovoCyte 1300), and NovoExpress software (Agilent, Santa Clara, USA) was used to analyze the flow cytometry data.

Cell migration and invasion assay

In total, 3×10^5 siRNA-treated SMMC-7721 or Hep3B cells were seeded into the upper chambers of transwell plates (catalog No. 3422, 8 μ m aperture; Corning, Glendale, USA), which were pre-coated with or without 8-fold diluted Matrigel™ (catalog No. 356234; BD Biosciences, Sparks, USA) for invasion or migration assay. Then, 500 μ L medium containing 10% FBS was added to the lower chamber. After 24 h of incubation, 0.5% crystal violet (in PBS) was used to stain the migrated cells and the number of migrated cells was then counted in 3 random fields using ImageJ 1.52v.

Quantitative polymerase chain reaction

Total RNA was extracted from SMMC-7721 and Hep3B cells after siRNA treatment using the Total RNA Extraction

Table 2. The primers of quantitative polymerase chain reaction (qPCR)

Name	Sequence 5'-3'	NCBI reference sequence
TMED5-F	AGAAGGAGTGCTTCTACCAGCC	NM_016040
TMED5-R	CTAAGGTTTTGCCTTCTGGAGAG	
18S-F	ACCCGTTGAACCCCATTCGTGA	NR_003286
18S-R	GCCTCACTAAACCATCCAATCGG	
MAPK1-F	ACACCAACCTCTCGTACATCGG	NM_002745
MAPK1-R	TGGCAGTAGGTCTGGTGCTCAA	
CDC14A-F	TAGATGGCAGCACACCCAGTGA	NM_033312
CDC14A-R	GTCCTGTCTTCCAAGACCAG	
mTOR-F	AGCATCGGATGCTTAGGAGTGG	NM_004958
mTOR-R	CAGCCAGTCATCTTTGGAGACC	
CDC27-F	ACACCTCTGTAATTGATGTGCC	NM_001256
CDC27-R	GGAGTTACCTCTCGGCTATTTC	
ROCK1-F	GAAACAGTGTCCATGCTAGACG	NM_005406
ROCK1-R	GCCGCTTATTTGATTCCTGCTCC	
CREBBP-F	AGTAACGGCACAGCCTCTCAGT	NM_004380
CREBBP-R	CCTGTCGATACAGTGCTTCTAGG	
CDC7-F	GGAAACTGCCAGTTCTTGCCC	NM_003503
CDC7-R	GGCACTTTGTCAAGACCTCTGG	
PIK3CA-F	GAAGCACCTGAATAGGCAAGTCG	NM_006218
PIK3CA-R	GAGCATCCATGAAATCTGGTCCG	

F – forward primer; R – reverse primer; TMED5 – transmembrane P24 trafficking protein; MAPK1 – mitogen-activated protein kinase 1; CDC – cell division cycle; mTOR – mammalian target of rapamycin; ROCK1 – Rho-associated coiled-coil containing protein kinase 1; CREBBP – cyclic adenosine monophosphate response element binding protein; PIK3CA – phosphatidylinositol-4,5-bisphosphate 3-kinase catalytic subunit alpha; NCBI – National Center for Biotechnology Information.

Reagent (catalog No. R401-01; Vazyme), and was used to synthesize complementary deoxyribonucleic acid (cDNA) using the HiScript II One-Step reverse transcriptase (RT)-PCR Kit (catalog No. P611-01; Vazyme). Quantitative polymerase chain reaction was then performed using the cDNA with a SYBR® Premix Ex Taq™ II (Takara, Kusatsu, Japan) and AriaMx Real-Time PCR System (Agilent), as previously described.¹⁰ The primers for qPCR are listed in Table 2.

Western blotting analysis

Protein extraction from the siRNA-treated SMMC-7721 and Hep3B cells was performed using radioimmunoprecipitation (RIPA) lysis solution (catalog No. P0013C; Beyotime Biotechnology) containing protease inhibitors (catalog No. ST505; Beyotime Biotechnology). Total protein concentration was quantified using a bicinchoninic acid (BCA) protein concentration determination kit (catalog No. P0012S; Beyotime Biotechnology). Western blotting was performed as previously described.¹⁰ In brief, equal amounts of total protein were resolved using 10–12% sodium dodecyl sulfate-polyacrylamide gel electrophoresis (SDS-PAGE) and then transferred to a polyvinylidene fluoride (PVDF) membrane

Table 3. The antibodies for western blot analysis

Classification	Name	Manufacturer	Catalog No.	Dilution rate
Primary antibody	TMED5 antibody	Abcam	ab254795	1:1000
	GAPDH antibody	Proteintech	60004-1-Ig	1:10,000
Secondary antibody	HRP-conjugated goat anti-mouse IgG	Proteintech	SA00001-1	1:10,000
	HRP-conjugated goat anti-rabbit IgG	Proteintech	SA00001-2	1:10,000

TMED5 – transmembrane P24 trafficking protein; GAPDH – glyceraldehyde-3-phosphate dehydrogenase; HRP – horseradish peroxidase.

(Merck Millipore, Burlington, USA). After incubation with 5% skimmed milk, primary and secondary antibodies were applied and the membranes were visualized using enhanced chemiluminescence (ECL) (Thermo Fisher Scientific, Waltham, USA). The antibodies used are shown in Table 3.

Statistical analyses

All statistical analyses were performed using IBM SPSS software v. 22.0 (IBM Corp., Armonk, USA). The normality of data was determined using the Shapiro–Wilk test or the D’Agostino–Pearson test. The Mann–Whitney U test was performed for nonparametric data between the 2 groups. The Wilcoxon matched-pairs signed rank test was used to compare nonparametric data of matched samples. One-way analysis of variance (ANOVA), followed by Tukey’s test, was used to identify the significant differences among multiple groups. An F-test for equality of variances was performed to ensure equal variance of the 2 test groups. The proportionality of the hazard function was checked based on the Schoenfeld residuals. The Kaplan–Meier survival analysis was used to evaluate the cumulative survival probability. The Cox proportional hazards regression models were used to estimate the hazard ratio of TMED5 and HCC. The Student’s unpaired t-test was used to compare the differences between the 2 groups for parametric data. The statistical significance level was set at $p < 0.05$.

Results

TMED5 is highly expressed in hepatocellular carcinoma

To investigate the function of TMED5 in HCC, the bioinformatics analysis was conducted, and it was found that the transcription of TMED5 was higher in the HCC tissues than in the normal tissues (Fig. 1A,B). The analysis of paired tumor tissues and adjacent normal tissues from TCGA and Gene Expression Omnibus further indicated that TMED5 levels were higher in the tumor tissues than in the normal tissues (Fig. 1C,D). Intriguingly, TMED5 transcription levels were lower in some tumors (e.g., thyroid carcinoma, lung adenocarcinoma, lung squamous cell carcinoma, and cholangiocarcinoma) while higher in others (e.g., HCC, cervical squamous cell carcinoma,

endocervical adenocarcinoma, and stomach adenocarcinoma), suggesting that TMED5 plays distinct roles in tumors (Fig. 1E). Thereafter, the expression levels of TMED5 in HCC cell lines were analyzed. Both mRNA and protein levels of TMED5 were higher in HCC Hep3B, HepG2, SMMC-7721, and Huh7 cell lines than in the normal liver cells L-02 cells (Fig. 1F,G). Overall, TMED5 was highly expressed in HCC.

Overexpression of TMED5 is associated with HCC progression

According to the optimal OS threshold, the HCC patients in this study ($n = 339$) were divided into low and high TMED5 expression groups to study the clinical significance of TMED5 expression. There were no significant differences between the 2 groups in terms of age ($n = 339$, $p = 0.1900$), gender ($n = 339$, $p = 0.3780$), family history of cancer ($n = 339$, $p = 0.5910$), Ishak score ($n = 339$, $p = 0.7210$), histological grade ($n = 339$, $p = 0.5440$), living status ($n = 339$, $p = 0.0594$), disease status ($n = 339$, $p = 0.2560$), or Child–Pugh score ($n = 339$, $p = 0.0878$) (Table 4). In contrast, the overexpression of TMED5 was closely related to serum AFP ($n = 339$, $p = 0.0030$), vascular invasion ($n = 339$, $p = 0.0205$), TNM stage ($n = 339$, $p = 0.0479$), and residual tumor ($n = 339$, $p = 0.0085$) (Table 4). These results indicate that TMED5 is positively associated with HCC progression.

Early hepatocellular carcinoma patients exhibiting high TMED5 levels had poor overall survival and disease-free interval

The Kaplan–Meier survival curve was used to analyze the relationship between TMED5 levels and OS or DFI in HCC patients. Patients with high TMED5 levels exhibited shorter OS (Fig. 2A). However, the level of TMED5 had no significant effect on patients’ DFI (Fig. 2B). It is worth noting that among HCC patients in TNM stages I and II, patients with high TMED5 levels had shorter OS and DFI than patients with low TMED5 levels, whereas for HCC patients in TNM stages III and IV, the relationship between TMED5 level and OS and DFI was not significant (Fig. 2C–F). These data demonstrate that high levels of TMED5 indicate a poor prognosis for HCC patients in TNM stages I or II. In addition, the multivariate analysis showed that TNM stages III (hazard ratio (HR) = 2.1, 95%

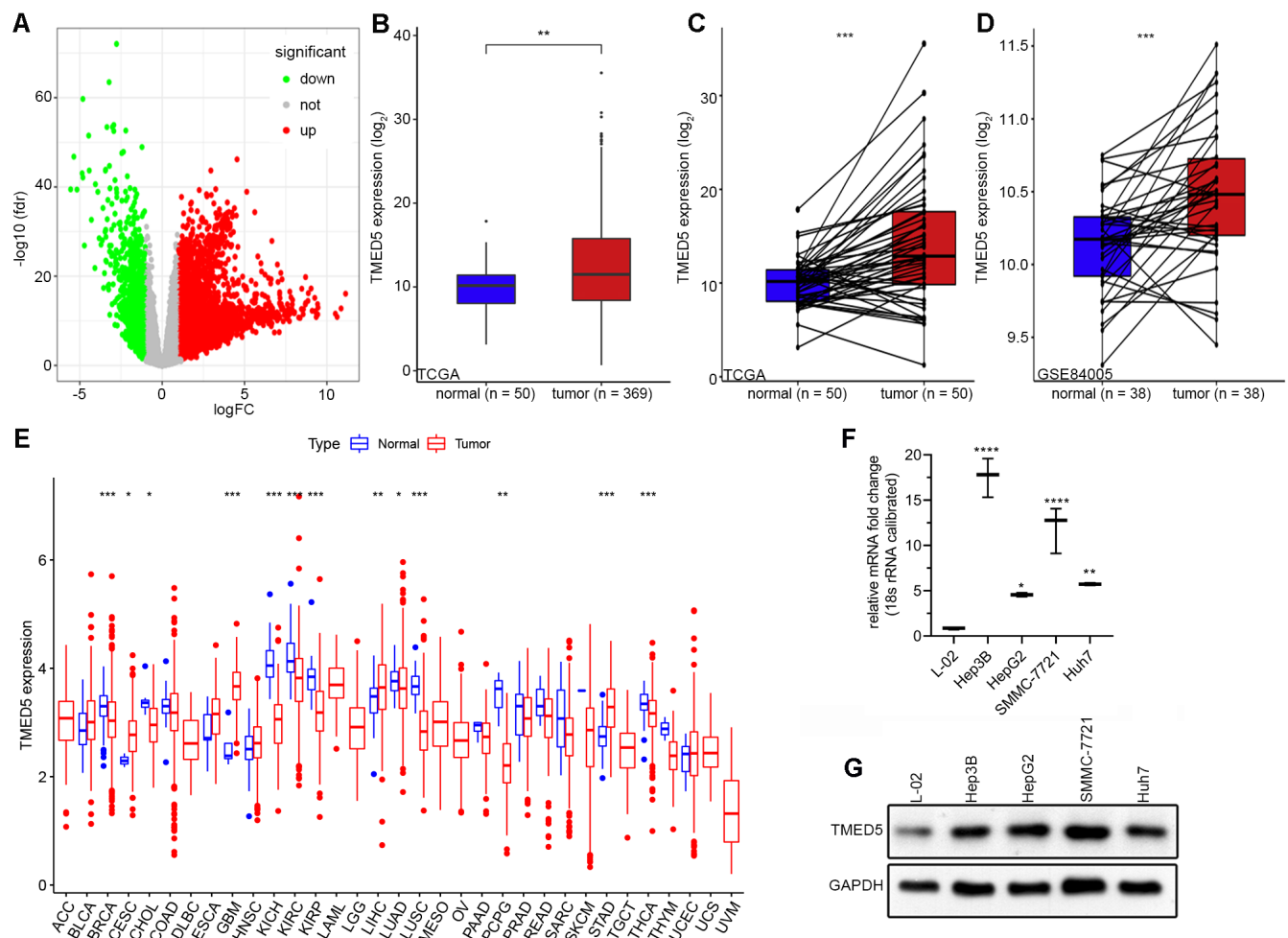


Fig. 1. Transcriptional levels of transmembrane P24 trafficking protein (TMED5) were higher in hepatocellular carcinoma (HCC) tissues than in adjacent normal tissues. A. Volcano map of gene expression in HCC tissues; B. The difference in TMED5 mRNA levels between HCC tissue (n = 369) and adjacent normal tissue (n = 50). The Mann–Whitney U test was used to analyze the data; C,D. The difference in TMED5 mRNA levels between HCC tissues and paired adjacent normal tissues from The Cancer Genome Atlas (TCGA) (C) or Gene Expression Omnibus (GSE84005) (D). The data were analyzed using the Wilcoxon matched-pairs signed rank test; E. The difference in TMED5 mRNA levels between distinct tumor tissues and corresponding adjacent normal tissues. The Mann–Whitney U test was used to analyze the data; F,G. Differences in TMED5 mRNA (F) and protein (G) levels between HCC cell lines and normal liver cell lines. All experiments were repeated independently 3 times. One-way analysis of variance (ANOVA) followed by the Tukey's test was used for statistical analysis. Box plots indicate the outliers, the maximum, the minimum, the medians, the upper quartile (Q1), and the lower quartile (Q3). Outliers are defined as values that lie 1.5 times beyond the interquartile range (IQR) above Q3 and below Q1. The maximum is defined as 1.5 times the IQR above Q3. The minimum is defined as 1.5 times the IQR below Q1

* $p < 0.05$; ** $p < 0.01$; *** $p < 0.001$; **** $p < 0.0001$.

confidence interval (95% CI) = 1.23–3.6, $p = 0.0060$) and IV (HR = 5.64, 95% CI = 1.73–18.43, $p = 0.0040$) could be considered as independent prognostic indicators of OS, whereas the TMED5 level was not an independent prognostic indicator of OS (Table 5).

The nomogram and calibration curve revealed the prognostic value of TMED5 in HCC patients

To explore the prognostic value of TMED5 levels in HCC patients, TMED5 mRNA levels and TNM stage were combined to plot nomograms. The nomogram and calibration curve showed excellent consistency between predicted postoperative survival rates (1-, 3- and 5-year OS and

DFI) and observed survival rates (1-, 3- and 5-year OS and DFI; Fig. 3). The C-indices for predicting OS and DFI were 0.6173 (95% CI: 0.5887–0.6458) and 0.6403 (95% CI: 0.6137–0.6668), respectively.

Downregulation of TMED5 expression inhibited cell proliferation, migration and invasion, and enhanced apoptosis

To verify the role of TMED5 in HCC, the effect of TMED5 on HCC cell proliferation, apoptosis, migration, and invasion of SMMC-7721 and Hep3B cells was investigated, as they expressed the highest levels of TMED5. Three siRNAs of TMED5, namely siTMED5-1, siTMED5-2 and siTMED5-3, were designed. Quantitative

Table 4. Relationship between transmembrane P24 trafficking protein (TMED5) expression and the clinical parameters of patients with hepatocellular carcinoma (HCC)

Characteristics	Level	TMED5 expression			p-value ^a
		Total (n = 339)	High (n = 217)	Low (n = 122)	
Age [years]	<65	208 (61.4%)	127 (58.5%)	81 (66.4%)	0.1900
	≥65	131 (38.6%)	90 (41.5%)	82 (66.4%)	
Gender	male	231 (68.1%)	152 (70.0%)	79 (64.8%)	0.3780
	female	108 (31.9%)	65 (30.0%)	43 (35.2%)	
Family history of cancer	no	196 (57.8%)	121 (55.8%)	75 (61.5%)	0.5910
	yes	98 (28.9%)	66 (30.4%)	32 (26.2%)	
	unknown	45 (13.3%)	30 (13.8%)	15 (12.3%)	
TNM stage	I	170 (50.1%)	100 (46.1%)	70 (57.4%)	0.0479
	II	84 (24.8%)	57 (26.3%)	27 (22.1%)	
	III	81 (23.9%)	59 (27.2%)	22 (18.0%)	
	IV	4 (1.2%)	1 (0.5%)	3 (2.5%)	
Histologic grade	G1–G2	212 (62.5%)	134 (61.8%)	78 (63.9%)	0.5440
	G3–G4	125 (36.9%)	81 (37.3%)	44 (36.1%)	
	unknown	2 (0.6%)	2 (0.9%)	0 (0%)	
Ishak score	0–4	124 (36.6%)	76 (35.0%)	48 (39.3%)	0.7210
	5–6	74 (21.8%)	48 (22.1%)	26 (21.3%)	
	unknown	141 (41.6%)	93 (42.9%)	48 (39.3%)	
Child–Pugh score	A	207 (61.1%)	123 (56.7%)	84 (68.9%)	0.0878
	B–C	21 (6.2%)	15 (6.9%)	6 (4.9%)	
	unknown	111 (32.7%)	79 (36.4%)	32 (26.2%)	
Vascular invasion	none	193 (56.9%)	120 (55.3%)	73 (59.8%)	0.0205
	micro	84 (24.8%)	48 (22.1%)	36 (29.5%)	
	macro	14 (4.1%)	9 (4.1%)	5 (4.1%)	
	unknown	48 (14.2%)	40 (18.4%)	8 (6.6%)	
Alpha fetoprotein	negative	143 (42.2%)	91 (41.9%)	52 (42.6%)	0.0030
	positive	120 (35.4%)	66 (30.4%)	54 (44.3%)	
	unknown	76 (22.4%)	60 (27.6%)	16 (13.1%)	
Residual tumor	R0	301 (88.8%)	189 (87.1%)	112 (91.8%)	0.0085
	R1–R2	12 (3.5%)	5 (2.3%)	7 (5.7%)	
	unknown	26 (7.7%)	23 (10.6%)	3 (2.5%)	
Living status	alive	224 (66.1%)	135 (62.2%)	89 (73.0%)	0.0594
	dead	115 (33.9%)	82 (37.8%)	33 (27.0%)	
Disease status	no	163 (48.1%)	98 (45.2%)	65 (53.3%)	0.2560
	yes	132 (38.9%)	87 (40.1%)	45 (36.9%)	
	unknown	44 (13.0%)	32 (14.7%)	12 (9.8%)	

^a χ^2 test; TNM – tumor-node-metastasis.

polymerase chain reaction and western blotting analysis showed that siTMED5-3 had the best knockdown efficiency (Fig. 4A,B).

The results of the MTT assay indicated that *TMED5* silencing significantly inhibited cell viability ($n = 3$, $p < 0.0001$; Fig. 4C). At the same time, cell cycle analysis revealed that *TMED5* silencing induced G_0/G_1 -phase arrest. Indeed, the percentage of cells in the G_0/G_1 phase increased from $28.387 \pm 0.830\%$ to $42.363 \pm 1.699\%$ ($n = 3$, $p = 0.0002$), and from $25.963 \pm 1.930\%$ to $39.217 \pm 1.522\%$ ($n = 3$, $p = 0.0007$), for SMMC-7721 and Hep3B cells, respectively (Fig. 4D). Moreover, *TMED5* silencing suppressed colony formation, as the number of colonies was reduced from 336.000 ± 15.000 to 138.667 ± 16.653 ($n = 3$, $p = 0.0001$) for SMMC-7721 cells, and from 127.667 ± 15.631 to 46.000 ± 9.539 ($n = 3$, $p = 0.0015$) for Hep3B cells (Fig. 4E).

The *TMED5* silencing significantly increased the percentage of apoptotic cells ($5.433 \pm 0.905\%$ compared to $14.650 \pm 1.760\%$, $p = 0.0013$, for SMMC-7721; $6.550 \pm 0.462\%$ compared to $14.127 \pm 2.865\%$, $n = 3$, $p = 0.0106$, for Hep3B; Fig. 4F). Finally, the effect of *TMED5* on cell migration was investigated. As shown in Fig. 5A,B, the *TMED5* silencing reduced the number of migrated SMMC-7721 cells from 547.000 ± 12.728 to 330.000 ± 11.518 ($n = 4$, $p < 0.0001$), and the number of migrated Hep3B cells from 426.500 ± 14.201 to 225.750 ± 16.741 ($n = 4$, $p < 0.0001$). Moreover, the number of invasive cells was reduced from 138.750 ± 15.903 to 62.500 ± 10.970 ($n = 4$, $p = 0.0002$) for SMMC-7721 cells, and from 132.750 ± 17.443 to 47.750 ± 7.588 ($n = 4$, $p = 0.0001$) for Hep3B cells (Fig. 5C,D). Taken together, these findings imply that *TMED5* is involved in the proliferation, apoptosis and metastasis of HCC cells.

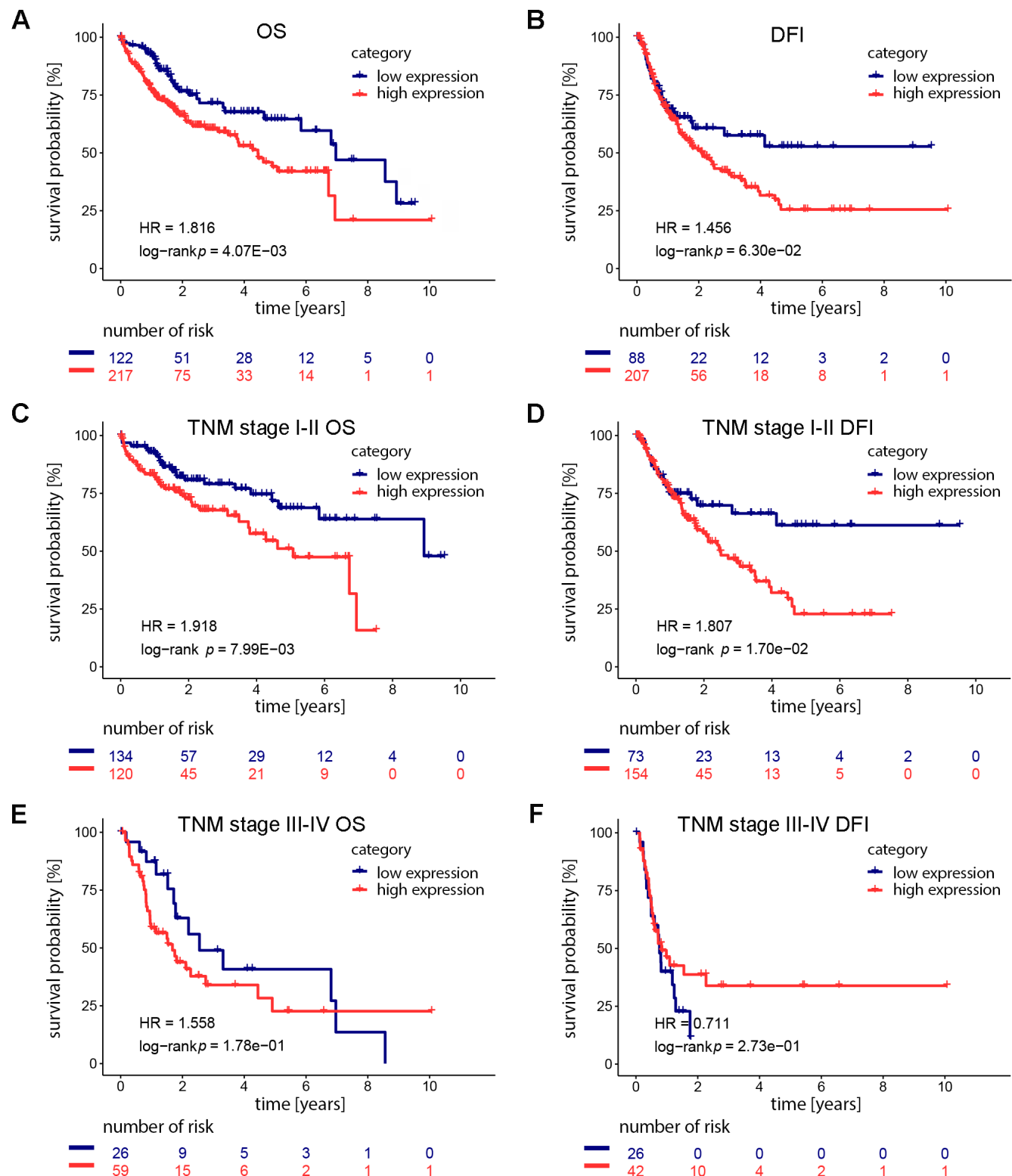


Fig. 2. Correlation between transmembrane P24 trafficking protein (TMED5) levels and overall survival (OS) and disease-free interval (DFI) in hepatocellular carcinoma (HCC) patients. A,B. The correlation between TMED5 levels and OS (A) or DFI (B) in all HCC patients was analyzed using the Kaplan–Meier (KM) curve; C,D. The correlation between TMED5 levels and OS (C) or DFI (D) in HCC patients at tumor-node-metastasis (TNM) stage I and II was analyzed using the KM curve; E,F. The correlation between TMED5 levels and OS (E) or DFI (F) in HCC patients at TNM stage I and II was analyzed using the KM curve. The log-rank test was used for statistical analysis.

HR – hazard ratio.

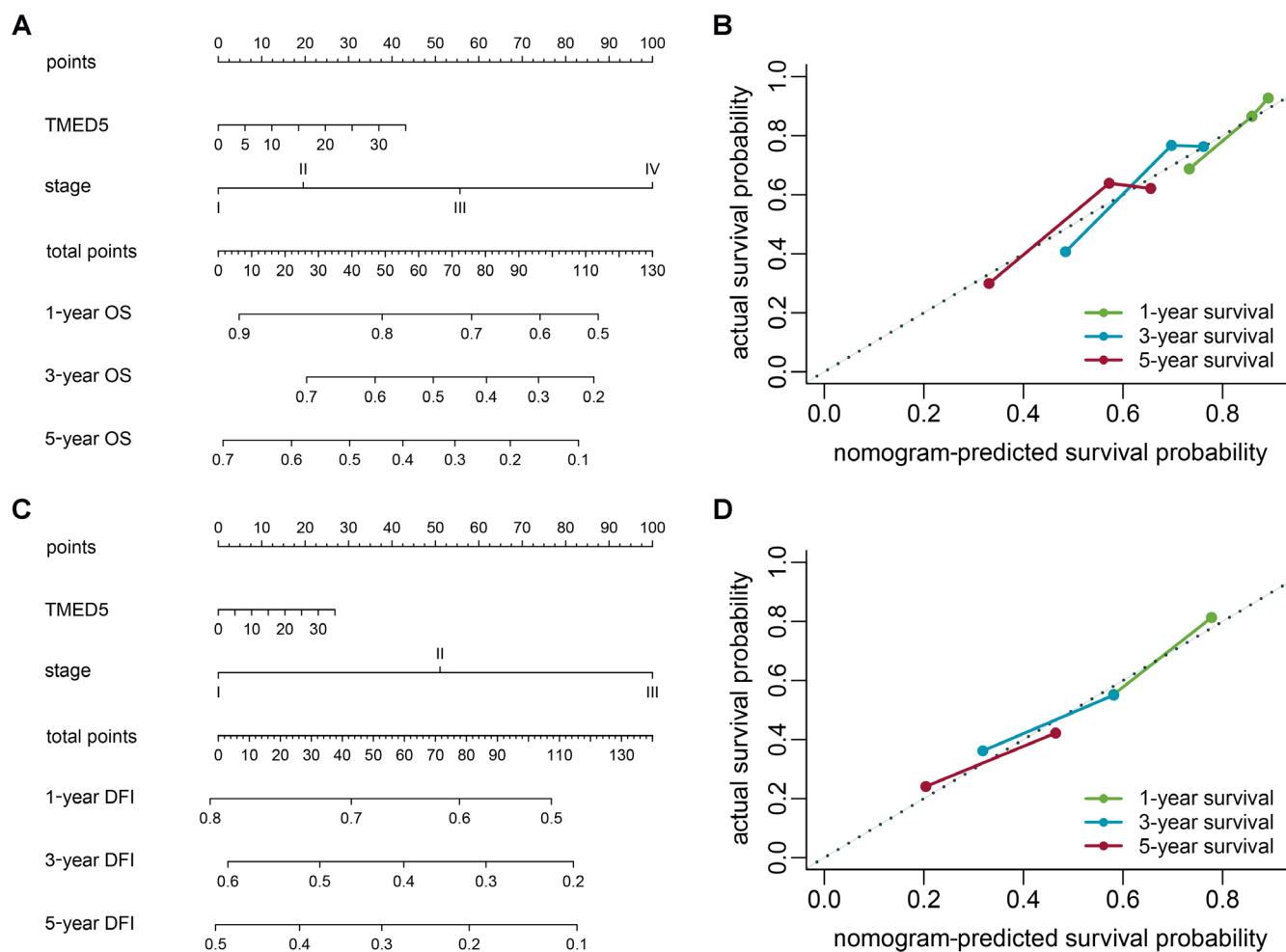


Fig. 3. Nomogram and calibration curve for hepatocellular carcinoma (HCC) patients to predict overall survival (OS) and disease-free interval (DFI). A,B. The 1-, 3- and 5-year OS in HCC patients predicted using nomogram (A) and calibration curve (B); C,D. The 1-year, 3-year, and 5-year DFI in HCC patients predicted using nomogram (C) and calibration curve (D)

TMED5 – transmembrane P24 trafficking protein.

Table 5. Cox proportional hazards regression model analysis of overall survival

Variables	Univariate analysis		Multivariate analysis	
	HR (95% CI)	p-value	HR (95% CI)	p-value
Age (≥ 65 years vs. < 65 years)	1.23 (0.85–1.78)	0.273	–	–
Gender (female vs. male)	1.26 (0.87–1.84)	0.228	–	–
Family history of cancer (yes vs. no)	1.14 (0.76–1.69)	0.530	–	–
TNM stage (II vs. I)	1.42 (0.87–2.32)	0.160	1.22 (0.65–2.29)	0.5360
TNM stage (III vs. I)	2.72 (1.78–4.15)	< 0.001	2.1 (1.23–3.6)	0.0060
TNM stage (IV vs. I)	5.44 (1.68–17.63)	0.005	5.64 (1.73–18.43)	0.0040
Histologic grade (G3–G4 vs. G1–G2)	1.14 (0.78–1.67)	0.489	–	–
Ishak score (5–6 vs. 0–4)	0.87 (0.5–1.5)	0.612	–	–
Child–Pugh score (B–C vs. A)	1.66 (0.82–3.36)	0.159	–	–
Vascular invasion (micro vs. none)	1.16 (0.72–1.88)	0.539	1.02 (0.59–1.79)	0.9360
Vascular invasion (macro vs. none)	2.52 (1.14–5.58)	0.023	2 (0.88–4.56)	0.0990
Alpha fetoprotein (positive vs. negative)	1.45 (0.92–2.28)	0.108	–	–
Residual tumor (R1–R2 vs. R0)	1.17 (0.43–3.2)	0.754	–	–
TMED5 (high vs. low)	1.1 (0.85–1.43)	0.472	–	–

Proportionality of hazard function was checked based on the Schoenfeld residuals. HR – hazard ratio; 95% CI – 95% confidence interval; TNM – tumor-node-metastasis.

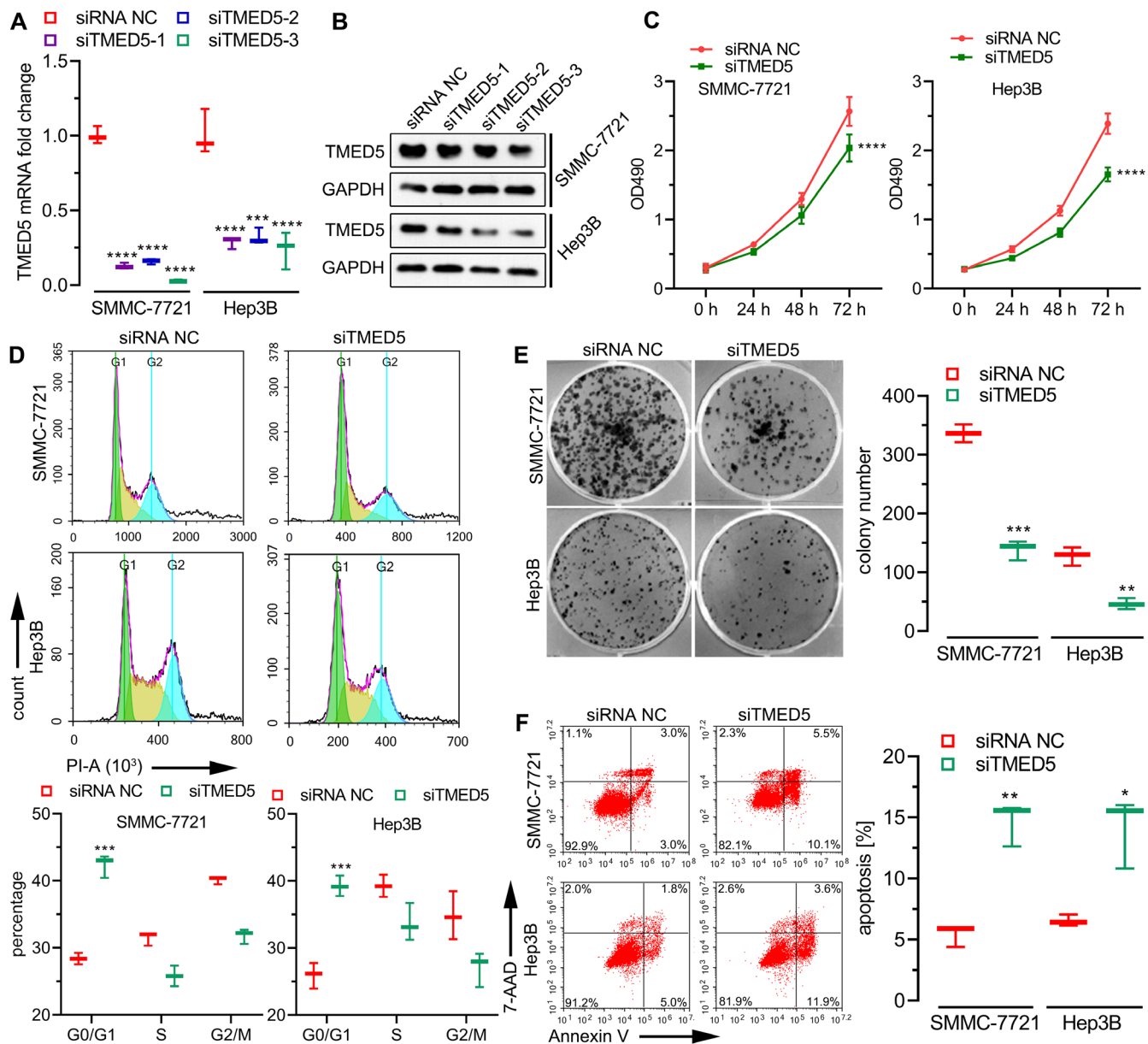


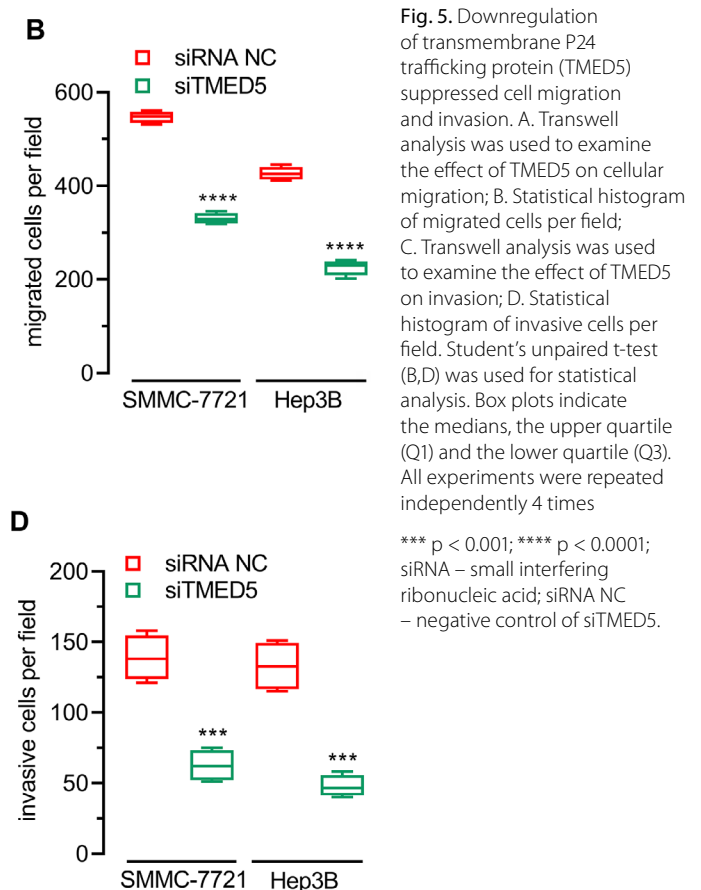
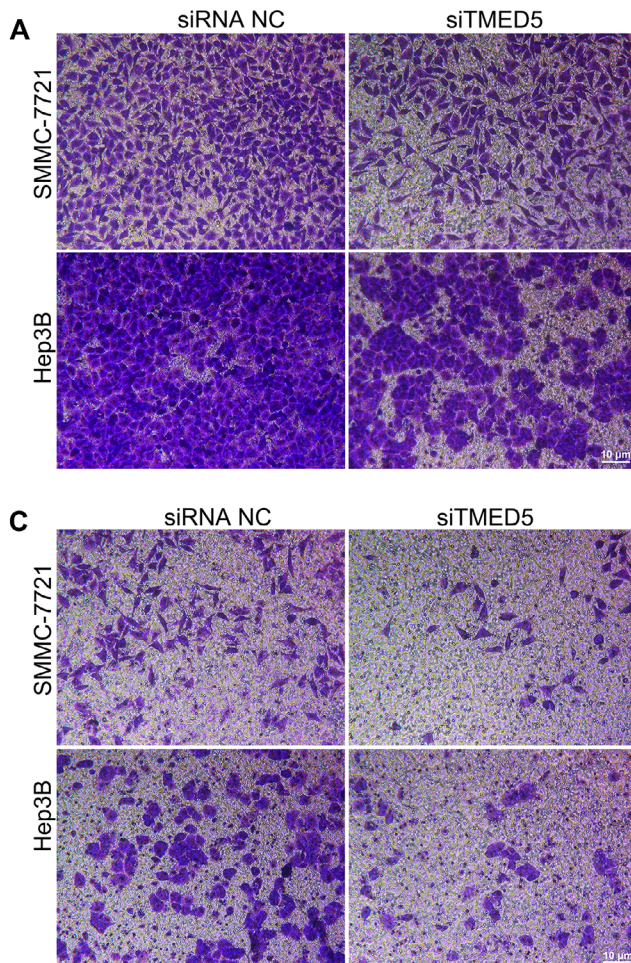
Fig. 4. Downregulation of transmembrane P24 trafficking protein (TMED5) inhibited cell proliferation and enhanced apoptosis. **A.** Quantitative polymerase chain reaction (qPCR) was used to detect the effect of siTMED5-1-, siTMED5-2- and siTMED5-3-mediated knockdown of *TMED5* in cells; **B.** Western blotting was used to detect the effect of siTMED5-1-, siTMED5-2- and siTMED5-3-mediated knockdown of *TMED5* in cells; **C.** MTT assay was used to detect the effect of the knockdown of *TMED5* on cell proliferation; **D.** The effect of *TMED5* downregulation on the cell cycle was determined; **E.** The effect of *TMED5* on colony formation was examined using a colony formation assay; **F.** Annexin V-fluorescein isothiocyanate (FITC) and 7-aminoactinomycin D (7-AAD) staining was used to detect the effect of *TMED5* on apoptosis. One-way analysis of variance (ANOVA) followed by the Tukey's test (**A**), and the Student's unpaired t-test (**C–F**) were used for statistical analysis. Box plots indicate the medians, the upper quartile (Q1) and the lower quartile (Q3). All experiments were repeated independently 3 times.

* $p < 0.05$; ** $p < 0.01$; *** $p < 0.001$; **** $p < 0.0001$; siRNA – small interfering ribonucleic acid; siRNA NC – negative control of siTMED5.

TMED5 levels positively correlated with the cell cycle, the mammalian target of rapamycin signaling pathway and the TGF- β signaling pathway

To explore the potential biological function of *TMED5* upregulation in HCC, GSEA was performed. This highlighted significant enrichment of the cell cycle, the mammalian target of rapamycin (mTOR) signaling pathway and the transforming growth factor beta (TGF- β) signaling

pathway (Fig. 6A,B). Moreover, genes co-expressed with *TMED5* in HCC samples with complete mRNA and sequencing data were evaluated and validated by silencing *TMED5* in SMMC-7721 and Hep3B cells. The *TMED5* silencing resulted in a decrease in both mRNA and protein levels of ras homolog enriched in brain (RHEB), cell division cycle 14A (CDC14A), structural maintenance of chromosomes 1A (SMC1A), cell division cycle 27 (CDC27), mitogen-activated protein kinase 1 (MAPK1), mTOR, ribosomal protein S6 kinase A3 (RPS6KA3),



phosphatidylinositol-4,5-bisphosphate 3-kinase catalytic subunit alpha (PIK3CA), stromal antigen 2 (STAG2), zinc finger FYVE domain containing 16 (ZFYVE16), origin recognition complex subunit 1 (ORC1), cyclic adenosine monophosphate response element binding protein (CREBBP), cell division cycle 7 (CDC7), cullin 1 (CUL1), Rho-associated coiled-coil containing protein kinase 1 (ROCK1), and zinc finger FYVE domain containing 9 (ZFYVE9), all of which are associated with the cell cycle, mTOR signaling or TGF- β signaling (Fig. 6C,D).^{11–26}

Discussion

Effective early diagnosis is essential to improve the survival rate of HCC patients.⁴ Some genes are useful in the diagnosis and treatment of HCC, including *AFP*, heat shock protein (*HSP*), glypican-3 (*GPC-3*), Golgi protein 73 (*GP73*), Des- γ -carboxy prothrombin (*DCP*), γ -glutamyl transferase (*GGT*), *TGF- β 1*, vascular endothelial growth factor (*VEGF*), microRNA-21 (*miRNA-21*), *miRNA-29*, *miRNA-199*, and *miRNA-500*.^{4,27,28} However, it is still necessary to further understand the occurrence of, and mechanisms underlying, the development of HCC

to improve its diagnosis and treatment. In this study, it was found that high transcriptional levels of TMED5 in HCC tissues were associated with poor OS in patients, suggesting that TMED5 is involved in HCC progression.

The Golgi apparatus, which is an essential organelle for protein transport and secretion, plays an important role in cellular life.²⁹ Also, there are many pro-apoptotic factors and mitosis-related molecules in the Golgi membrane.²⁹ Several stimuli that promote cell death cause fragmentation of the Golgi apparatus and the subsequent induction of apoptosis and autophagy.²⁹ Therefore, Golgi function has a fundamental impact on the survival of cancer cells,²⁹ which indicates that the Golgi apparatus is a potential target for anticancer therapies. The TMED5 is a component of the Golgi apparatus essential for its maintenance and acts in the early stages of the secretory pathway.⁶ However, studies investigating the role of TMED5 in cancer are limited. Yang et al. revealed that TMED5 was upregulated in cervical cancer cells and promoted nuclear autophagy and malignant behavior,⁷ suggesting that TMED5 may play an important role in the progression of cancer. In this study, TMED5 promoted proliferation and metastasis but suppressed apoptosis in HCC cells, indicating that *TMED5* serves as an oncogene in HCC. Nevertheless, the molecular

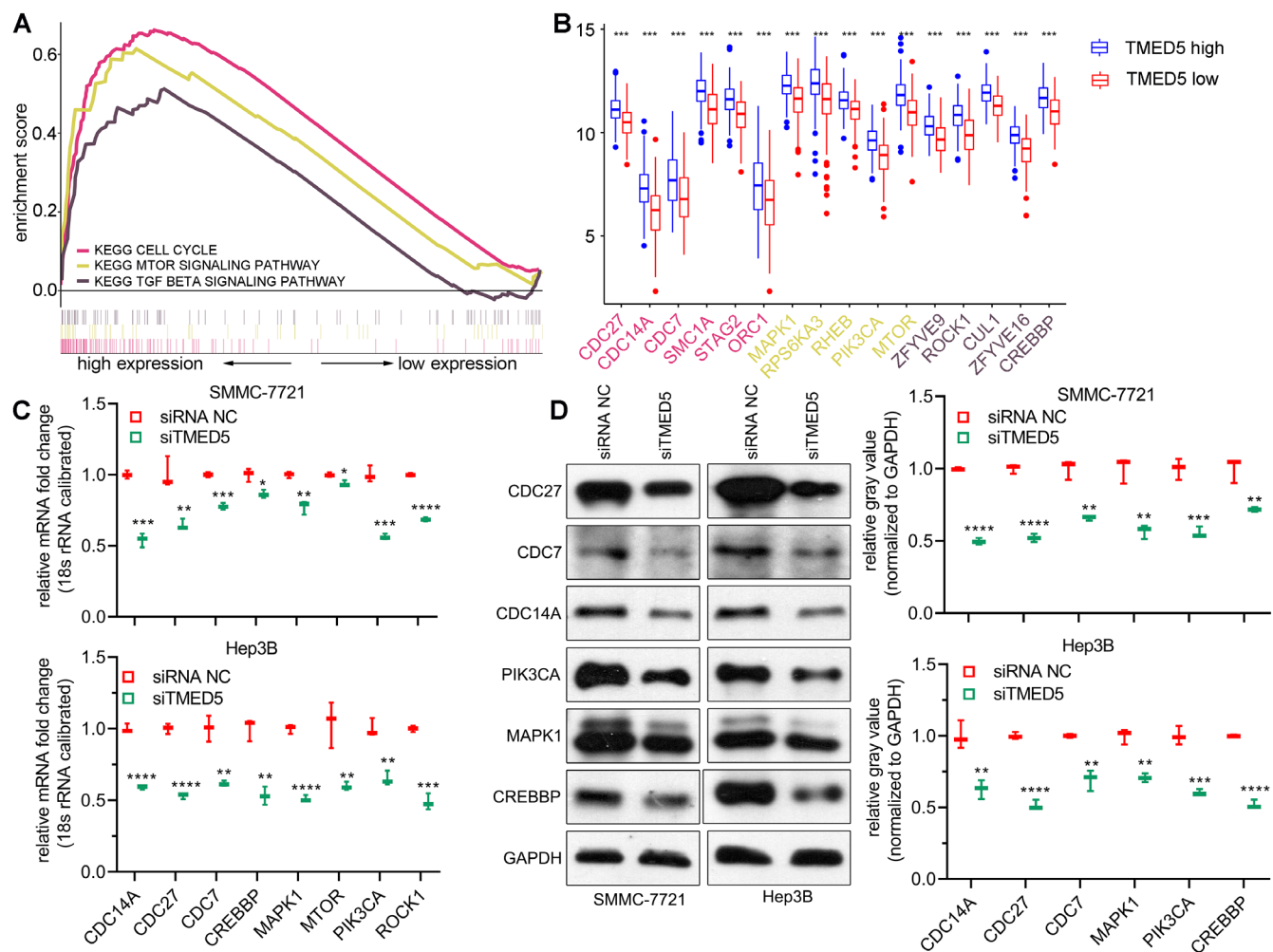


Fig. 6. Transmembrane P24 trafficking protein (TMED5) was positively correlated with the cell cycle, the mammalian target of rapamycin (mTOR) signaling pathway and the tumor growth factor beta (TGF- β) signaling pathway. **A.** The activation gene sets related to the cell cycle, mTOR signaling pathway and TGF- β signaling pathway are shown in the gene set enrichment analysis (GSEA) enrichment curve; **B.** The correlation between the expression of genes related to the cell cycle, mTOR signaling pathway and TGF- β signaling pathway, and the expression of TMED5 in HCC; **C,D.** The expression of CDC14A, CDC27, MAPK1, mTOR, PIK3CA, CREBBP, CDC7, and ROCK1 after *TMED5* silencing in SMMC-7721 and Hep3B cells. Mann-Whitney U test (**B**) and Student's unpaired t-test (**C**) were used for statistical analysis. Box plots indicate the outliers, the maximum, the minimum, the medians, the upper quartile (Q1), and the lower quartile (Q3). Outliers are defined as values that lie 1.5 times beyond the interquartile range (IQR) above Q3 and below Q1. The maximum is defined as 1.5 times the IQR above Q3. The minimum is defined as 1.5 times the IQR below Q1. All experiments were performed independently 3 times

* $p < 0.05$; ** $p < 0.01$; *** $p < 0.001$; **** $p < 0.0001$.

mechanism by which TMED5 promotes HCC progression is still unknown. We have shown that *TMED5* knockdown reduced the expression level of genes including *RHEB*, *CDC14A*, *SMC1A*, *CDC27*, *MAPK1*, *mTOR*, *RPS6KA3*, *PIK3CA*, *STAG2*, *ZFYVE16*, *ORC1*, *CREBBP*, *CDC7*, *CUL1*, *ROCK1*, and *ZFYVE9*, all of which are involved in cell cycle progression, mTOR signaling or TGF- β signaling,^{11–26} and whose abnormalities are closely related to the pathogenesis of cancers.^{30–32}

A previous study had revealed that TMED5 was up-regulated by MIR-G-1 (a type of miRNA) in cervical cancer cells in a G-rich RNA sequence binding factor 1 (GRSF1)-dependent manner, which promoted nuclear autophagy, malignant behavior and interaction with Wnt

family member 7B (WNT7B), thereby activating the classic WNT-catenin beta 1 (CTNNB1)/ β -catenin signaling pathway.⁷ However, whether TMED5 promotes the transcription of the aforementioned genes through the activation of the WNT7B/ β -catenin signaling pathway or other signaling pathways needs further investigation.


Limitations


Limitations of this study include the lack of animal experiments to further verify the findings. The detailed mechanism of action of TMED5 in the cell cycle, mTOR signaling pathway and TGF- β signaling pathway also require further investigation.


Conclusions


This study demonstrated that high transcriptional levels of TMED5 in HCC tissues were related to poor OS in HCC patients. Moreover, the downregulation of TMED5 expression in HCC cells inhibited proliferation, migration and invasion, and enhanced apoptosis. As such, TMED5 is a potential regulator of the cell cycle, mTOR signaling pathway and TGF- β signaling pathway, and has the potential to promote HCC.


ORCID iDs


Xianyi Cheng  <https://orcid.org/0000-0003-4265-6916>

Xiulan Deng  <https://orcid.org/0000-0003-3214-006X>

Huiping Zeng  <https://orcid.org/0000-0001-8567-4810>

Tao Zhou  <https://orcid.org/0000-0003-1547-0462>

Dezhi Li  <https://orcid.org/0000-0002-4500-7439>

Wei V. Zheng  <https://orcid.org/0000-0002-8942-1543>

References

- Sagnelli E, Macera M, Russo A, Coppola N, Sagnelli C. Epidemiological and etiological variations in hepatocellular carcinoma. *Infection*. 2020;48(1):7–17. doi:10.1007/s15010-019-01345-y
- Waller LP. Hepatocellular carcinoma: A comprehensive review. *World J Hepatol*. 2015;7(26):2648–2663. doi:10.4254/wjh.v7.i26.2648
- Zhao YJ, Ju Q, Li GC. Tumor markers for hepatocellular carcinoma. *Mol Clin Oncol*. 2013;1(4):593–598. doi:10.3892/mco.2013.119
- Tak H, Kang H, Ji E, Hong Y, Kim W, Lee EK. Potential use of TIA-1, MFF, microRNA-200a-3p, and microRNA-27 as a novel marker for hepatocellular carcinoma. *Biochem Biophys Res Commun*. 2018;497(4):1117–1122. doi:10.1016/j.bbrc.2018.02.189
- Li D, Zhang J, Li J. Role of miRNA sponges in hepatocellular carcinoma. *Clin Chim Acta*. 2020;500:10–19. doi:10.1016/j.cca.2019.09.013
- Koegler E, Bonnon C, Waldmeier L, Mitrovic S, Halbeisen R, Hauri HP. p28, a novel ERGIC/cis Golgi protein, required for Golgi ribbon formation. *Traffic*. 2010;11(1):70–89. doi:10.1111/j.1600-0854.2009.01009.x
- Yang Z, Sun Q, Guo J, et al. GRSF1-mediated MIR-G-1 promotes malignant behavior and nuclear autophagy by directly upregulating TMED5 and LMNB1 in cervical cancer cells. *Autophagy*. 2019;15(4):668–685. doi:10.1080/15548627.2018.1539590
- Scaravilli M, Asero P, Tammela TL, Visakorpi T, Saramäki OR. Mapping of the chromosomal amplification 1p21-22 in bladder cancer. *BMC Res Notes*. 2014;7(1):547. doi:10.1186/1756-0500-7-547
- Goldman M, Craft B, Swatloski T, et al. The UCSC Cancer Genomics Browser: Update 2015. *Nucleic Acids Res*. 2015;43(D1):D812–D817. doi:10.1093/nar/gku1073
- Xu X, Zheng S. MiR-887-3p negatively regulates STARD13 and promotes pancreatic cancer progression. *Cancer Manag Res*. 2020;12:6137–6147. doi:10.2147/CMAR.S260542
- Jin L, Williamson A, Banerjee S, Philipp I, Rape M. Mechanism of ubiquitin-chain formation by the human anaphase-promoting complex. *Cell*. 2008;133(4):653–665. doi:10.1016/j.cell.2008.04.012
- Yazdi PT, Wang Y, Zhao S, Patel N, Lee EYHP, Qin J. SMC1 is a downstream effector in the ATM/NBS1 branch of the human S-phase checkpoint. *Genes Dev*. 2002;16(5):571–582. doi:10.1101/gad.970702
- Imtiaz A, Belyantseva IA, Beirl AJ, et al. CDC14A phosphatase is essential for hearing and male fertility in mouse and human. *Hum Mol Genet*. 2018;27(5):780–798. doi:10.1093/hmg/ddx440
- Sancak Y, Bar-Peled L, Zoncu R, Markhard AL, Nada S, Sabatini DM. Regulator-Rag complex targets mTORC1 to the lysosomal surface and is necessary for its activation by amino acids. *Cell*. 2010;141(2):290–303. doi:10.1016/j.cell.2010.02.024
- Wortzel I, Seger R. The ERK cascade: Distinct functions within various subcellular organelles. *Genes Cancer*. 2011;2(3):195–209. doi:10.1177/1947601911407328
- Cheng X, Ma X, Zhu Q, et al. Pacer is a mediator of mTORC1 and GSK3-TIP60 signaling in regulation of autophagosome maturation and lipid metabolism. *Mol Cell*. 2019;73(4):788–802.e7. doi:10.1016/j.molcel.2018.12.017
- Zhou Y, Yamada N, Tanaka T, et al. Crucial roles of RSK in cell motility by catalysing serine phosphorylation of EphA2. *Nat Commun*. 2015;6(1):7679. doi:10.1038/ncomms8679
- Di Donato N, Rump A, Mirzaa GM, et al. Identification and characterization of a novel constitutional PIK3CA mutation in a child lacking the typical segmental overgrowth of PIK3CA-related overgrowth spectrum. *Hum Mutat*. 2016;37(3):242–245. doi:10.1002/humu.22933
- Prieto I, Pezzi N, Buesa JM, et al. STAG2 and Rad21 mammalian mitotic cohesins are implicated in meiosis. *EMBO Rep*. 2002;3(6):543–550. doi:10.1093/embo-reports/kvf108
- Seet LF, Liu N, Hanson BJ, Hong W. Endofin recruits TOM1 to endosomes. *J Biol Chem*. 2004;279(6):4670–4679. doi:10.1074/jbc.M311228200
- Tocilj A, On KF, Yuan Z, et al. Structure of the active form of human origin recognition complex and its ATPase motor module. *eLife*. 2017;6:e20818. doi:10.7554/eLife.20818
- Iyer-Bierhoff A, Krogh N, Tessarz P, Ruppert T, Nielsen H, Grummt I. SIRT7-dependent deacetylation of fibrillarin controls histone H2A methylation and rRNA synthesis during the cell cycle. *Cell Rep*. 2018;25(11):2946–2954.e5. doi:10.1016/j.celrep.2018.11.051
- Montagnoli A. Drf1, a novel regulatory subunit for human Cdc7 kinase. *EMBO J*. 2002;21(12):3171–3181. doi:10.1093/emboj/cdf290
- Scott DC, Rhee DY, Duda DM, et al. Two distinct types of E3 ligases work in unison to regulate substrate ubiquitylation. *Cell*. 2016;166(5):1198–1214.e24. doi:10.1016/j.cell.2016.07.027
- Niemann MCE, Bartrina I, Ashikov A, et al. Arabidopsis ROCK1 transports UDP-GlcNAc/UDP-GalNAc and regulates ER protein quality control and cytokinin activity. *Proc Natl Acad Sci U S A*. 2015;112(1):291–296. doi:10.1073/pnas.1419050112
- Lin HK, Bergmann S, Pandolfi PP. Cytoplasmic PML function in TGF- β signalling. *Nature*. 2004;431(7005):205–211. doi:10.1038/nature02783
- Arai T, Kobayashi A, Ohya A, et al. Assessment of treatment outcomes based on tumor marker trends in patients with recurrent hepatocellular carcinoma undergoing trans-catheter arterial chemo-embolization. *Int J Clin Oncol*. 2014;19(5):871–879. doi:10.1007/s10147-013-0634-6
- Asaoka Y, Tateishi R, Nakagomi R, et al. Frequency of and predictive factors for vascular invasion after radiofrequency ablation for hepatocellular carcinoma. *PLoS One*. 2014;9(11):e111662. doi:10.1371/journal.pone.0111662
- Migita T, Inoue S. Implications of the Golgi apparatus in prostate cancer. *Int J Biochem Cell Biol*. 2012;44(11):1872–1876. doi:10.1016/j.biocel.2012.06.004
- Phan TG, Croucher PJ. The dormant cancer cell life cycle. *Nat Rev Cancer*. 2020;20(7):398–411. doi:10.1038/s41568-020-0263-0
- Ayuk SM, Abrahamse H. mTOR signaling pathway in cancer targets photodynamic therapy in vitro. *Cells*. 2019;8(5):431. doi:10.3390/cells8050431
- Colak S, ten Dijke P. Targeting TGF- β signaling in cancer. *Trends Cancer*. 2017;3(1):56–71. doi:10.1016/j.trecan.2016.11.008